

Novel Technology on Synthesizing Mg-Zn Biomaterial Using Arc Plasma Sintering

Marzuki Silalahi¹, Henni Sitompul², Jojor Lamsihar Manalu^{3,*}, Kiagus Dahlan⁴, Deni Noviana⁵, Arbi Dimiyati¹

¹ Centre for Science and Technology of Advanced Materials, National Nuclear Energy Agency, Indonesia

² Dept. of Physics, STKIP SURYA, Surya Institute, Indonesia

³ Department of Physiology, Medical Faculty, Atma Jaya University, Indonesia

⁴ Dept. of Physics, Faculty of Mathematics and Natural Sciences, Bogor Agricultural University, Indonesia

⁵ Dept. of Veterinary Clinic Reproduction and Pathology, Faculty of Veterinary, Bogor Agricultural University, Indonesia

*Corresponding author's email: manalujojorlamsihar [AT] gmail.com

ABSTRACT--- *In this work the development of new sintering technology using plasma which is generated by DC-Arc for synthesizing of biomaterial based on MgZn is reported. Magnesium alloy is suited as implant material due to its young modulus which is close to natural bone and bio-compatible with the human body. The MgZn biomaterial is composed of Mg and Zn powder in 94:6 ratio of weight. The mixture was ball milled for four hours, and then isostatic pressed at 570 MPa to form a coin of 1.5 cm in diameter. The coin was subsequently consolidated in the Arc Plasma Sintering (APS) for 30 seconds. For this experiment the APS was operated at 12 Volts and 1 Amps. As comparison, one sample coin was sintered in a conventional furnace at temperature of 350 °C for one hour. The formed MgZn alloys were characterized by using X-Ray Diffraction (XRD) and Scanning Electron Microscopy equipped with an Energy Dispersive X-ray spectroscopy (SEM-EDX). The result showed the sample sintered in APS exhibits high homogeneity with lattice parameter slightly smaller than sample sintered in the furnace. It can be an indication to the higher solubility of Zn in Mg matrix processed in APS. The 6 wt.% Zn addition formed MgZn alloys in the form of solid solution with smaller distance of crystal planes. Synthesizing of MgZn biomaterial can be performed using APS in short time and low energy.*

1. INTRODUCTION

The role of MgZn alloy for treatment of bone fracture becomes more and more important mainly due to its biocompatibility, low cost and relatively large availability of raw materials. The major advantage of MgZn as biomaterial are that it could easily self destroyed and dissolve completely in body tissue [1, 2, 3, 4]. Moreover, Magnesium (Mg) has the Young's Modulus between 41-45 GPa little higher to those of the natural bone (3-20 GPa) than to those of iron (ca.211,4 GPa) or zink (ca. 90 GPa) [3, 5]. Zn is the important substance and could quick degrade in human body. MgZn alloy shows good mechanical properties suitable for application as human bone [2, 5, 6]. MgZn alloy could be synthesized both by melting and casting [7,8] and by sintering process [9, 10]. However, because of its low melting point the production of MgZn alloy through these conventional techniques is very susceptible to oxidation.

The aim of this work is to test a new technology for synthesis of biomaterial based on MgZn by using plasma heat in arc plasma sintering (APS). APS can be controlled relatively precise to be operated at very low energy down to 12 Watt. As comparison, some samples were produced by conventional technique using electrical furnace. SEM and XRD analysis were used in order to get insight into the process during the MgZn alloy formation.

2. EXPERIMENTALS

The materials used for the experiment are Mg and Zn powder of 99.8 % purity from Aldrich. MgZn alloys were obtained by mixing Mg and Zn powder with a weight ratio 94 : 6. The mixture was then homogenized in a ball milling for 4 hours. The Mg-Zn mixtures are and compacted in a dye 1.5 cm of diameter using uniaxial compacting machine at a pressure of 570 MPa to get green pellet coin. The sintering processes were performed both in the APS and in a conventional furnace. Sintering process with APS was conducted in an argon gas environment to avoid oxidation. The APS was operated at the 12 Volts and 1 Amperes with exposure time 30 seconds. On the other hand, during sintering in the conventional furnace the sample pellet was air tight capsulated in a quartz glas. The sintering was performed at a temperature 350 °C for 1 hour.

After APS and conventional sintering both samples were then characterized using X-ray Diffraction (XRD) at range of 2θ of 25°-80°. The phase identification was done using the software High Score Expert and the Full Width at

Half Maximum (FWHM) calculation was performed using the software Match 2.2.1. The morphology of sintered pellet was identified using Scanning Electron Microscopy (SEM) which is equipped with Energy-Dispersive X-Ray Spectroscopy (EDX). The XRD and SEM-EDX characterization was done at National Nuclear Energy Agency (BATAN) at Serpong, Tangerang Selatan

3. RESULTS AND DISCUSSIONS

3.1 Microstructure of MgZn Alloy

Figure 1 shows the SEM micrographs of Mg and Zn particles as received. It can be seen in Figure 1a that Mg particles exhibit plate like shapes and their size is obviously larger than Zn particles. Figure 2b (taken at magnification of 2000x) shows that Zn particles are homogeneously distributed over the Mg particles after 4 hours ball milling which occupy the Mg particles surface rifts.

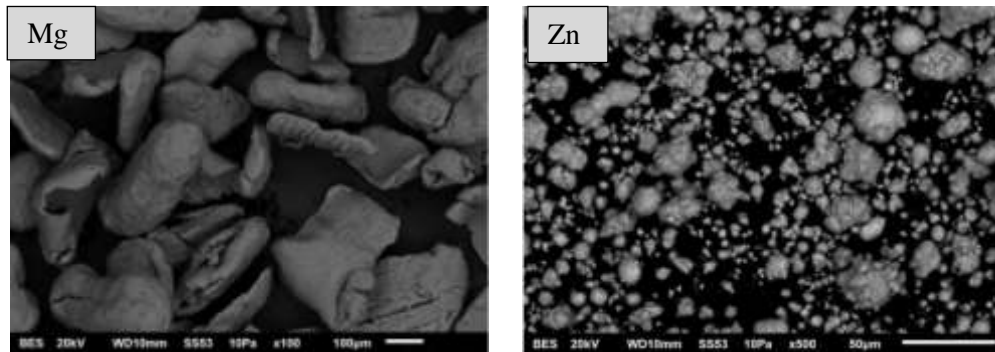


Figure 1. SEM micrographs of Mg and Zn powders as received.

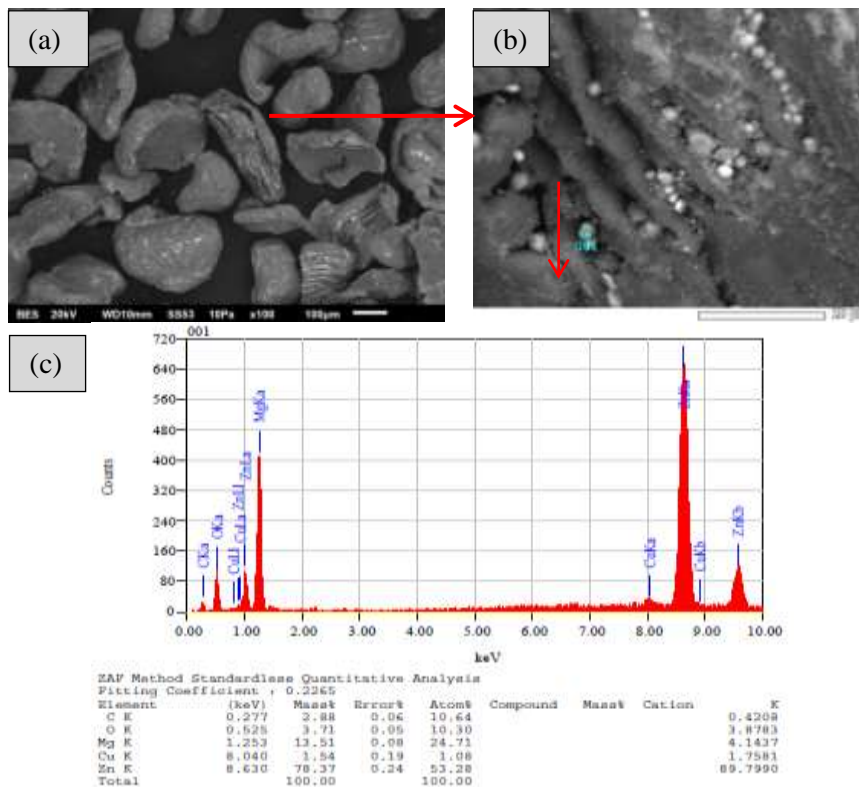


Figure 2. SEM micrographs of Mg-Zn mixture after 4 hours of ball milling process (a-b) and its corresponding EDX spectrum (c).

The SEM micrographs and EDX spectrum of MgZn alloy after APS sintering process are showed in Figure 3. Figure 3(a) shows the presence of Zn precipitation in form of small dendrites which are found along the grain boundaries as obvious by the white color. The Zn dendrite formation indicates that the plasma temperature has exceeded the melting point of Zn. So that during the sintering Zn has probably completely melted which during cooling process forms characteristic dendrites structures. The EDX result in figure 3b confirms that the alloy grains consist of 97 wt.% Mg and 3

wt.% Zn. This means that part of Zn has been homogenously dissolved in Mg matrix. The solubility limit of Zn in Mg alloy was reported to be 6.2 wt.% at 340 °C [5].

The MgZn alloy microstructure sintered in electrical furnace is shown in Figure 4. In contrast to that observed in the sample produced by using APS no dendritic Zn precipitations can be found in the alloys after conventional sintering. This can be interpreted that the sintering temperature was low which was below the melting point of Zn. This result is in fully agreement with the microstructure of MgZn alloy that reported by Paliwal and Ho Jung earlier [12]. Based on EDX spectrum and the MgZn phase diagram it can be concluded that the bright colors (position 2 and 3 in Figure 4) constitute to the Zn which occupies almost the alloy grain boundaries. This results shows that Zn only present in the grain boundaries, some of them forms agglomeration as showed Figure 4 position 3. The matrix constitutes of single element Mg.

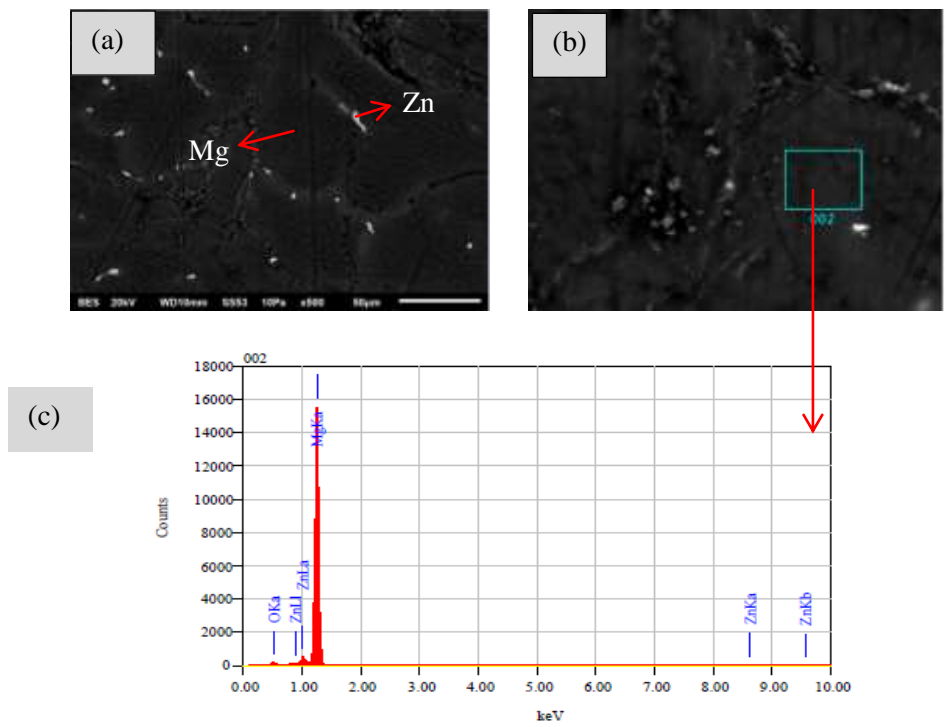


Figure 3. SEM micrographs of MgZn alloy after APS sintering process (a-b) and EDX spectrum of the Mg matrix as indicated by the square mark.

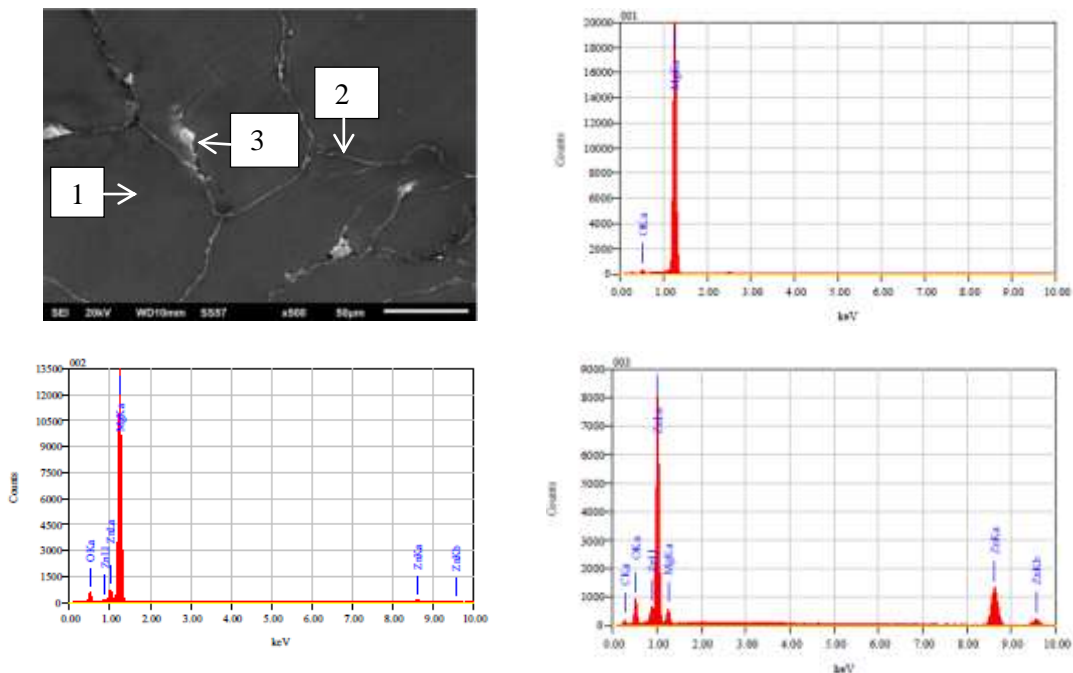


Figure 4. SEM micrograph of MgZn alloy after sintering in the electrical furnace and its corresponding EDX spectren.

3.2 Phase of MgZn Alloy

Figure 5 shows the XRD diffraction patterns of the Mg, Zn and Mg-Zn powder before sintering process. Diffraction pattern of Mg-Zn mixture (green color) is clearly a combination of the diffraction pattern of Mg (blue color) and Zn (red color), in which the maximum peak Zn is visible on the position 2θ of 43° .

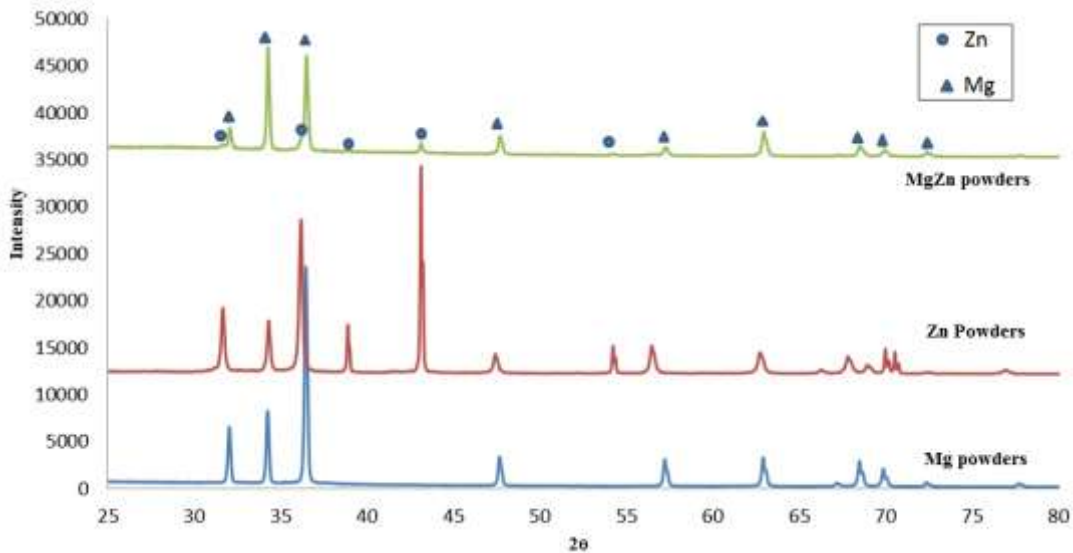


Figure 5. XRD diffraction patterns for powders of Mg, Zn and mixture of Mg-Zn before sintering process.

The diffraction pattern of Mg-Zn mixture after sintering process using APS and Furnace showed in Figure 6. It can be seen that there is no new peaks appearing after sintering process using neither APS nor Furnace. It seems to be there is no new phase formed after the both sintering processes. The Mg peak pattern correspond with previous studies reported by Jojor for matrix Mg [11]. However, in more detailed view, there are shifting of Mg peaks to the right for both of sintering methods APS and Furnace and reducing the Zn peaks intensity (even a Zn peak missing) after the sintering process.

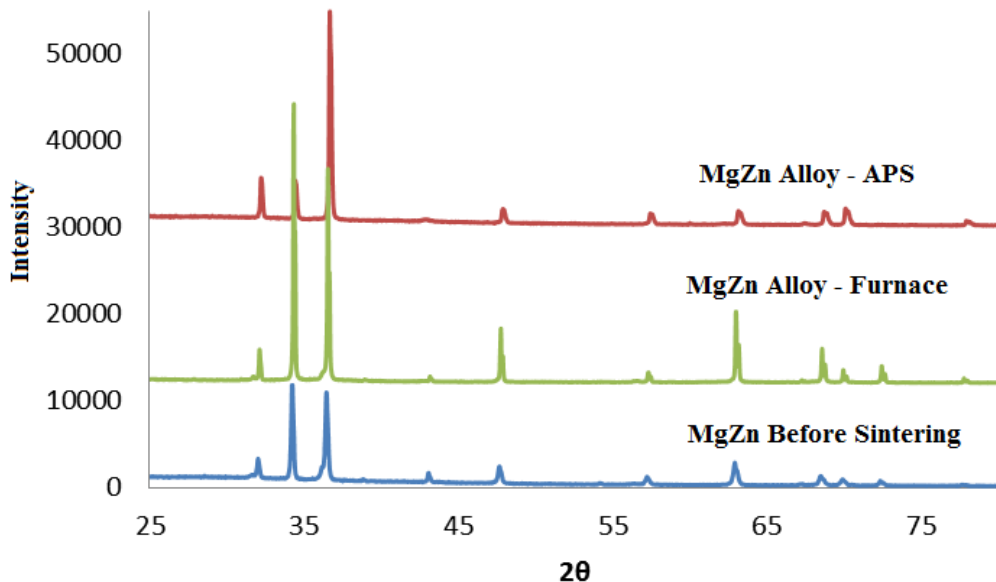


Figure 6 XRD diffraction patterns for MgZn before sintering process, after APS sintering process, and after Furnace sintering process.

The shifting of Mg peaks can be clearly seen in Figure 7. This behaviour can be interpreted that some Zn atoms have been dissolved and replaced some Mg atoms in their lattices that may change the distance between the crystal planes Mg. Based on the Bragg law, the distance between the crystal planes (d) is inversely proportional to diffraction

angle (θ), therefore the diffraction pattern which is shifted to the right (of grater 2θ) indicates the distance between the crystal planes (d) is getting smaller. The distance reduction of crystal planes is caused by the Zn atom radius that smaller than Mg atoms. The crystal system of Mg becomes shrivelled due to atomic shifting during atomic substitution process. Dissolution of Zn into Mg is also confirmed by the reduction in Zn peak intensity after the sintering process, as shown in Figure 8. Shifting of Mg peaks and reducing Zn peak intensity after process of sintering showed that the MgZn alloy has been successfully synthesized using either APS or Furnace. There is no new phase other than solid solution MgZn alloy. These results are corresponding to MgZn phase diagram as shown at [13].

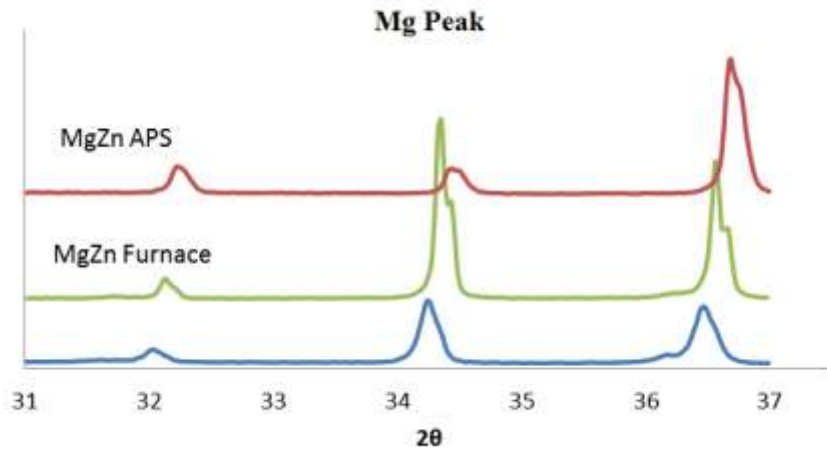


Figure 7 The shifted peak pattern of Mg at MgZn alloy diffraction pattern.

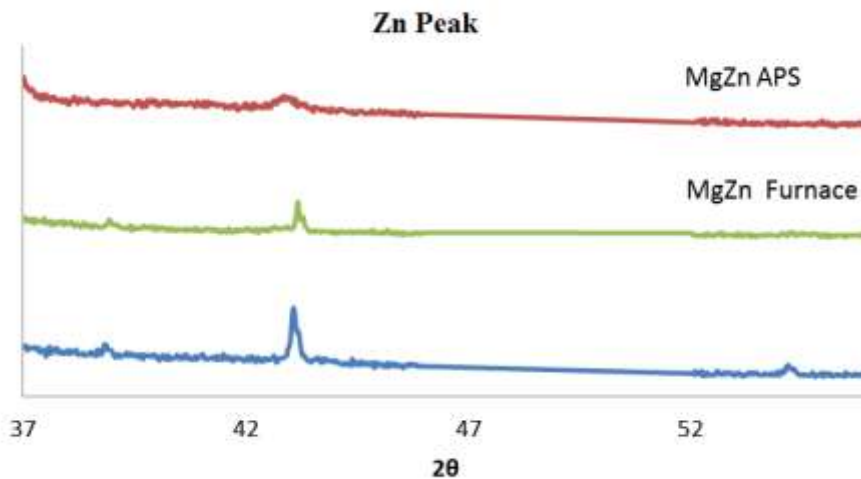


Figure 8. The decreasing peak intensity of Zn at MgZn alloy diffraction pattern after APS sintering and electrical furnace sintering.

Further phase identification was done using software high score plus with ICSD database as shown in Table 1. From these results it is known that the alloy produced by either APS or furnace consists of two phases, Mg and Zn phase that both have the space group P63/mmc (194). Mg phase lattice parameters listed in Table 1 is the result of refining with the Chi square value of 4.708 for using APS sintering and of 1.875 for using furnace sintering. The lattice parameter of Mg of the alloy results using APS is smaller than that of sintering in the furnace, in other words the distance between the crystal field using APS is smaller. It is also seen in Figure 7. The smaller distance between the crystal planes of Mg indicating that more dissolved Zn in Mg, thus it can be said that the sintering process using APS can solve more Zn in Mg than using conventional furnace.

Tabel 1. Information of MgZn Alloy Phase.

Phase	Database		Lattice parameters of Alloy	
	APS	Furnace	APS	Furnace
Mg	ICSD 98-065-1728 a=b=3,2120 c=5,2150	ICSD 98-018-1728 a=b=3,2120 c=5,2150	a=b= 3,2049 c = 5,2046	a=b= 3,2086 c = 5,2096
	ICSD 98-042-1015 a=b=2,6700 c=5,0020	ICSD 98-065-3504 a=b=2,665 c=4,947	a=b= 2,6700 c=5,001999	a=b= 2,665 c =4,947

Table 2. Calculation of the crystallite size of MgZn before and after sintering process.

Treatments	Cutt of	$k\lambda/D$	D (Å)	D (nm)
MgZn before sintering	-5.7171	0.0032892	416.82781	41.68
MgZn Furnace sintering	-5.879	0.0027976	490.08224	49.01
MgZn APS sintering	-6.0356	0.0023921	573.16476	57.32

3.3 Crystallite Size of MgZn Alloy

Crystallite size of MgZn alloy that results on this study was calculated by Scherrer equation and Scherrer modification equation [13], as shown in Table 2. Crystallite size calculation is done for each treatment, where θ and FWHM values obtained from the analysis phase using Match 2.2.1 which is then converted to units of radians.

Based on Table 2, it can be seen that the MgZn alloy crystallites size are bigger after the APS sintering process. The large crystallite sizes indicate that the re-crystallization occurred during the heat treatment by sintering [14]. From this it can be seen that the sintering treatment using the APS has a higher temperature than the electrical furnace.

4. CONCLUSIONS

MgZn alloys have been successfully synthesized by sintering using either APS and electrical furnace. The MgZn alloy appears as a solid solution, Zn completely dissolved in the Mg matrix and caused the shrinkage of the Mg crystal plane distance. APS can be used for production of MgZn alloy with higher success for only 30 sec at very low energy. MgZn produced by this method exhibits high grade of alloying as obviously verified by the XRD result.

5. ACKNOWLEDGEMENT

The project was financially supported by the Ministry for Research, Technology and Higher Education under the SINas RT2016-0287 and by the Center for Science and Technology for Advanced Materials, Nuclear Energy Agency of Indonesia. The authors gratefully thank to Mr. Rohmad Salam for his help by operating Arc Plasma Sintering (APS) and Mr. Agus Sujatno for SEM analysis.

6. REFERENCES

- [1] Hermawan, Hendra 2012, *Biodegradable metals from concept to applications*, Springer Briefs in Materials.
- [2] Li H, Peng Q, Li X, Li K, Han Z, Fang D 2014, Microstructures, mechanical and cytocompatibility of degradable Mg-Zn based orthopedic biomaterials, *Material and Desain*, **58**:43-51.
- [3] Živić F, Grujović N, Manivasagam G, Richard C, Landoulsi J, Petrović V 2014, The potential of magnesium alloys as bioabsorbable/biodegradable implants for biomedical applications, *Tribology in Industry* **36**: 67-73.
- [4] Witte F. 2010, The history of Biodegradable magnesium implants: A review, *Acta Biomaterialia* **6**:1680–1692.
- [5] Chen Y, Xu Z, Smith C, Sankar J 2014, Recent advances on the development of magnesium alloys for biodegradable implants, *Acta Biomaterialia* **10**:4561–4573.

- [6] Salleh E M, Zuhailawati H, Ramakrishnan S, Gepreel MAH 2015, A statistical prediction of density and hardness of Biodegradable mechanically alloyed Mg–Zn alloy using fractional factorial design, *Journal of Alloys and Compounds* **644**: 476–484.
- [7] Xuenan Gu, Yufeng Zheng, Yan Cheng, Shengping Zhong, Tingfei Xi 2009, In vitro corrosion and biocompatibility of binary magnesium alloys, *Elsevier, biomaterials*, **30**,484- 498.
- [8] Telma Blanco Matias, Gabriel Hitoshi Asato, Bruno Torquato Ramasco, Walter José Botta, Claudio Shyinti Kiminami, Claudemiro Bolfarini, " Processing and characterization of amorphous magnesium based alloy for application in biomedical implants", elsevier, abm, *J Mater Res Technol.* 2014, **3(3)**:203-209.
- [9] N. Saheb, A S Hakeem, A Khalil, N Al-Aqeeli, T Laoui 2013, Synthesis and spark plasma sintering of Al-Mg-Zr alloys", Springer, *Journal of Central South University of Technology, Press and Springer, J. Cent. South Univ.* **20**: 7-14.
- [10] Eme Marina Salleh, Sivakumar Ramakrishnan, and Zuhailawati Hussain 2015, Synthesis of biodegradable Mg-Zn alloy by mechanical alloying:effect of milling time, *Science Direct, Procedia Chemistry* **19** (2016) 525 – 530 .
- [11] Manalu J L, Soegijono B, Indrani D J, Study of Mg-Hydroxyapatite Composite with various composition of Hydroxyapatite which obtained From Cow Bones in Simulation Body Fluid (SBF), *Asian Journal of Applied Sciences*, 2016, **(4)**: 810 - 816
- [12] Paliwal M, HoJung I 2014, Microstructural evolution in Mg–Zn alloys during solidification: An experimental and simulation study, *Journal of Crystal Growth* **394**:28–38.
- [13] Islam M M, Mustafa A O, Medraj M 2014, Essential magnesium alloy binary phase diagram and their thermochemical data *Journal of Materials* : 1-33.
- [14] Monshi A, Foroughi M R, Monshi M R 2012, Modified scherrer equation to estimate more accurately nano-crystallite size using XRD *World journal of nano science and engineering*, **2**:154-160.